

## Article

# DRASTIC Index GIS-Based Vulnerability Map for the Entre-os-Rios Thermal Aquifer

Vanessa Gonçalves <sup>1,2,3</sup> , Antonio Albuquerque <sup>1,2,3,\*</sup> , Pedro G. Almeida <sup>1,2</sup>  and Victor Cavaleiro <sup>1,2</sup>

<sup>1</sup> Department of Civil Engineering and Architecture, University of Beira Interior, Calçada Fonte do Lameiro 6, 6200-358 Covilha, Portugal

<sup>2</sup> GeoBioTec-UBI, University of Beira Interior, Calçada Fonte do Lameiro 6, 6200-358 Covilha, Portugal

<sup>3</sup> FibEnTech, University of Beira Interior, Calçada Fonte do Lameiro 6, 6200-358 Covilha, Portugal

\* Correspondence: antonio.albuquerque@ubi.pt; Tel.: +351-275-329-734

**Abstract:** The sulphurous mineral waters of ‘Entre-os-Rios’, which is sited in NW Portugal, are famous for their long history as thermal baths dating back at least to the mid-sixteenth century. Because of the singularity of its water composition, especially the highest sulphur content, the mineral waters of ‘Entre-os-Rios’ are one of the most important sulphurous waters in Portugal. Despite these mineral waters having a protection perimeter buffer zone to avoid water contamination, there are potentially damaging installations (e.g., fuel station) in the closed protection buffer zone that, according to existing law, are not permitted within the protection perimeters, which defeats the purpose of their delineation. A vulnerability map was created using geographic information system (GIS) tools based on multi-criteria analysis, combining thematic maps and parameters of the DRASTIC index, for evaluating the risk of contamination in the protection area. The results showed that within the perimeter, there was a low risk of pollution. The alluvium-covered terrain was vulnerable to moderate contamination, but it was far from the catchment point. Areas of minimal risk corresponded to locations where the granitic massif had not been significantly weathered. The map enables information collection for a better definition of local resource structures and planning, namely, for restricted areas emplacement where some activities should not be allowed (e.g., agriculture and water prospection), given its influence on the confined granitic aquifer.

**Keywords:** hydromineral resources; geographic information system; vulnerability map; protection perimeters; DRASTIC index



**Citation:** Gonçalves, V.; Albuquerque, A.; Almeida, P.G.; Cavaleiro, V. DRASTIC Index GIS-Based Vulnerability Map for the Entre-os-Rios Thermal Aquifer. *Water* **2022**, *14*, 2448. <https://doi.org/10.3390/w14162448>

Academic Editor: Frédéric Huneau

Received: 11 June 2022

Accepted: 2 August 2022

Published: 9 August 2022

**Publisher’s Note:** MDPI stays neutral with regard to jurisdictional claims in published maps and institutional affiliations.



**Copyright:** © 2022 by the authors. Licensee MDPI, Basel, Switzerland. This article is an open access article distributed under the terms and conditions of the Creative Commons Attribution (CC BY) license (<https://creativecommons.org/licenses/by/4.0/>).

## 1. Introduction

The world’s freshwater resource comprises groundwater and surface water, which are essential to human systems and ecosystems. Groundwater is a source of water that is widely used for supplying a variety of water demands. Mineral water is an excellent groundwater asset at local and regional levels, as well as a high-value resource due to its use in thermal medicinal baths [1–4]. Natural mineral waters (NMWs) are natural groundwater that originated from meteoric waters that infiltrated into the unsaturated zone and circulate underground via deep crustal discontinuities (e.g., major faults, shear zones), acquiring a distinct physical and chemical composition that results from water–rock interactions and temperature, which are constant over time; these waters are normally located in a singular geologic and morphotectonic framework and usually have a deep source [5–9]. Similarly, NMWs might be described as deep circulation waters with a specific bacteriological profile and physicochemical characteristics that are stable at their source within the range of natural fluctuations and have certain therapeutic or beneficial health effects [10,11].

Groundwater must satisfy severe standards to be classified as NMW. This water is the ‘noblest relative’ of groundwater [4]. The abundance of NMW and spring water in

Portugal has a high heritage value [11]. Thermal waters can be found throughout the world and are used for recreational and therapeutic purposes. Over the decades and across cultures, spas have played an important role in promoting community health. Portugal is a country that is rich in hydromineral resources, mostly in the form of alkaline sulphurous groundwater [3,4,12]. The mineral waters of ‘Entre-os-Rios’ are one of the most important sulphurous waters in Portugal due to the uniqueness of its water composition, particularly the highest sulphur level [3,9,12–14].

NMW has been used all over the world for recreational and therapeutic purposes [15–22] and has been playing an important role in promoting community health over the decades and across cultures [17,23]. The various therapeutic effects have been attributed to its physicochemical composition and this correlation has been the basis for the indication of different thermal resorts for different disorders of several vital systems of the body [24–26]. Instances of a ‘salus per aquam’ (spa) are often found in magnificent natural settings, where they contribute to the economic development of the communities and areas where they are present, and they are frequently the only source of income [4]. In recent years, there has been a growth in health consciousness due to the study of NMW and the establishment of spa businesses based on the concept of collaborative interaction between natural resources and man-made enterprises [20]. The spa industry is expected to be approximately USD 94 billion by 2025, with a steady expansion in the following decades. Indeed, the global wellness business has expanded both the demand and supply for products and services based on NMW [27].

This sort of water (mostly sulphury waters) is frequently associated with specific hydrogeological conditions, requiring the adjustment of territorial planning strategies for its preservation that consider the heritage, cultural, and scientific values to which it is linked. By establishing a protection perimeter buffer zone, the risk of groundwater contamination is reduced. If a pollution event occurs, corrective action should be taken promptly to avoid the water reaching the catchment with unacceptable levels of pollutants. Several point and non-point sources of pollutants from diverse land-use activities, such as agricultural fertilizer application, expanding urbanization, domestic wastewater infiltration, road runoff, solid waste landfills, wastewater ponds, mining ponds, and industrial effluents, could potentially contaminate aquifer systems, affecting the quality of the groundwater [28–33]. As a result of the contamination of surface water resources, groundwater demand is increasing year after year [34]. When aquifers become polluted, contamination is persistent and difficult to remediate due to its large storage, long residence times, physical inaccessibility, and monetary difficulties [35–38].

Since 1928, Portuguese legislation [39] has established protected buffer zones for NMWs, which can include three levels of protection, as presented in Figure 1. The delimitation of these zones integrates a resource management tool that aims to provide quantitative and qualitative information for water preservation.

Given the hydrogeological conditions, a wellhead protection area will be established, which will incorporate the following features: (i) an immediate protection buffer zone, where all activities not related to groundwater exploitation are prohibited (the corresponding area is normally protected by a fence); (ii) a closed protection buffer zone, where all activities or facilities that may contaminate the groundwater, whether via infiltration of contaminants or changing the flow paths, are prohibited or strictly controlled; and (iii) the distant protection buffer zone, where all activities are prohibited or strictly controlled.

The need to protect groundwater involves considering an aquifer’s vulnerability to pollution [40,41]. Groundwater vulnerability to pollution, according to the National Academies Press (NAP) [42], is defined as the tendency or likelihood for contaminants to reach a specific point in the groundwater system after being introduced above the uppermost aquifer. Within this concept, there are two types of vulnerability concepts [43,44]: (i) intrinsic vulnerability, which is determined by the aquifer’s hydrogeological characteristics (e.g., depth of the water table, recharge, hydraulic conductivity, saturated and unsaturated zone), and (ii) specific vulnerability, which includes a few outside variables in

addition to the hydrogeological characteristics (e.g., land occupation, sort of contaminant). It is possible that aquifers with high vulnerability, but a low pollution risk exist due to the absence of polluting loads, or that aquifers with a high pollution risk exist despite their low vulnerability [41].

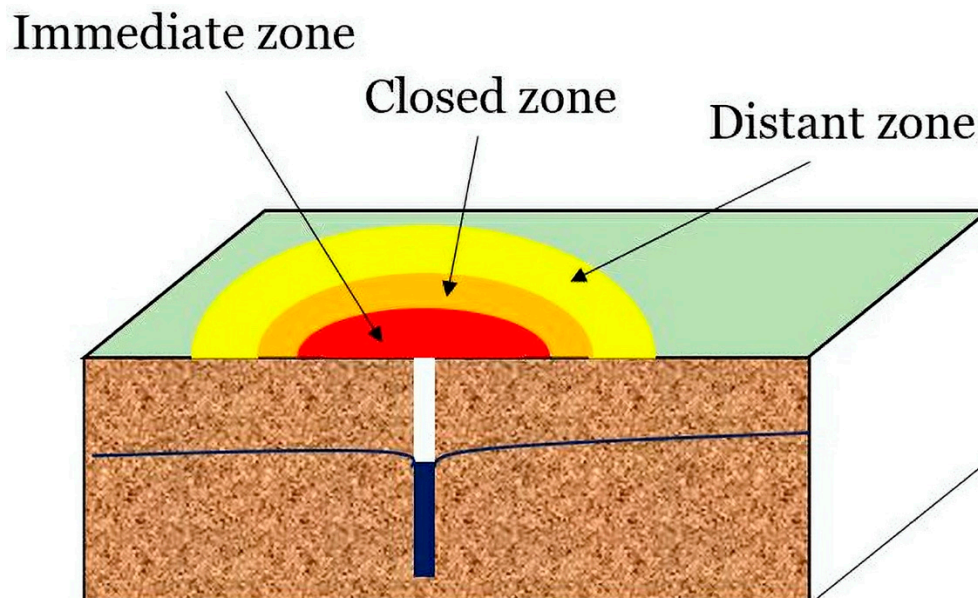


**Figure 1.** Schematic representation of the different protection buffer zones of a groundwater borehole (adapted from [39]).

Groundwater vulnerability assessment and mapping have developed as a central subject given the need for sustainable aquifer management [45–47]. The study of groundwater vulnerability allows for the identification of areas with the highest potential for contamination, as well as the creation of aquifer pollution vulnerability maps [37,38,46,48–50]. Groundwater pollution involves many factors (e.g., geological, geomorphological, climatic, biological), where some of these factors are particularly important for vulnerability mapping (e.g., geological materials, landforms, unsaturated zone, aquifer hydraulic features, land use) [36]. Given the issue's complexity, a variety of models, each with its vulnerability rating, statistical approaches, process-based methodologies, and overlay and index methods, are required [47]. Despite existing methodologies, there is no satisfactory way to represent aquifer vulnerability due to the difficulty in integrating all parameters that influence contaminant behaviour [51]. The DRASTIC model, whether applying the original index developed by Aller et al. [40] or its updated variations, is one of the most widely used tools for evaluating groundwater vulnerability within the framework of a geographic information system (GIS) environment [47,52–54].

The use of GIS has simplified the acquisition, processing, analysis, and manipulation of georeferenced data [47,55–61]. GIS-based model development has become critical for studies of groundwater vulnerability and quality using hydrogeological parameters and anthropogenic activities [62]. The creation of thematic maps allows for better planning and management, both in terms of sustainable water use and the demarcation of places with the ability (or not) to implement various activities based on their potential impact on aquifers [62–65]. Map algebra operations enable mathematical operations to be performed between several thematic charts, resulting in composite charts, typically of vulnerability or susceptibility of a spatial nature, as shown for environmental applications in [55–58].

Therefore, the main objective of this work was to create a vulnerability map for the 'Entre-os-Rios' thermal aquifer using GIS interpolation tools based on the DRASTIC index. It is reasonable to infer that the hydromineral resource may have been contaminated due to activities (like a fuel station) inside the closed zone. Additionally, we aimed to compare the areas specified by the current protective perimeter with the radius arbitrated

in accordance with the applicable legal requirements [39]. The main strategy was to provide a high-quality environmental data source for the region so that the DRASTIC index could be representative.

## 2. Materials and Methods

### 2.1. Study Area

The thermal aquifer is situated in ‘Lugar da Torre—Eja’, municipality of ‘Penafiel’, district of ‘Porto’ (NW Portugal), and the main research object of the study was the ‘Barbeitos’ borehole, which is in the ‘Maciço Antigo’ in the Douro Hydrographic Region where rivers converge. The importance of the ‘Entre-os-Rios’ thermal aquifer in the life and economy of this area goes back to the 1920s when the thermal complex was raised. The current agreement for the exploration of natural mineral water was signed in 1997 [63]. In 2003, law no. 203/2003 [64] defined the protection buffer zones for the ‘Barbeitos’ borehole (immediate, closed, and distant buffer zones) (Figure 2) based on parameters that support a sustainable exploration of the resource. The mineral water exploration concession has the registration number HM-23 and the name ‘Entre-os-Rios—Quinta da Torre’, with a surface area of 96.6 ha that is coincident with the closed protection buffer zone. The extended protection buffer zone covers an area of 241.8 ha.

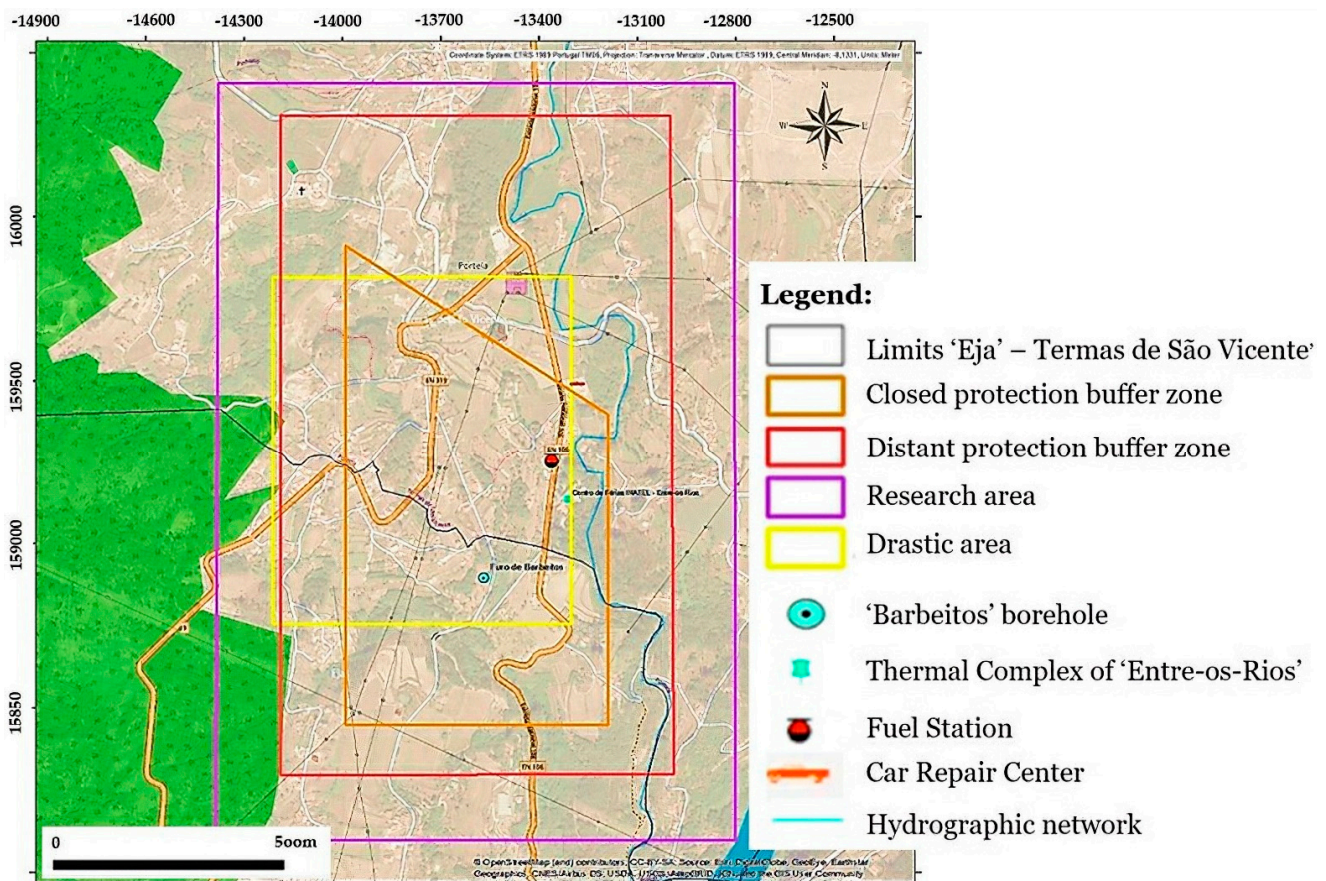


**Figure 2.** Location map of the ‘Barbeitos’ borehole and protection buffer zones and their conditions.

The region is part of the Iberian Massif’s Central Iberian Zone (CIZ) [66,67]. From a geomorphological standpoint, the region is shaped by a dense network of deeply settled watercourses that flow into the Douro river after drawing pathways that are quite sinuous [64]. The hilly blocks that separate the ‘Ribeira de Camba’, ‘Ribeira de Matos’, and ‘Ribeira das Lages’ define the straight path of the rivers. The arrangement in flat-topped stepped blocks, which are almost exclusively carved by the secondary hydrographic network, is determined by the ENE–WSW to SE–NW lineations [68]. The area is characterized by steep

slope variations (Figure 3), which are primarily due to the presence of Ordovician quartzite rocks, which gave rise to a NW–SE ridge orientation due to differential erosion. On a local scale, the massif is dominated by rock discontinuities, which are typically sub-vertical but can also be horizontal to sub-horizontal. Joints are usually crushed and weathered, revealing an important structural control [64,68]. As a result of their adaptation to crushing fault bands, watercourses have a geometric layout [63,67].

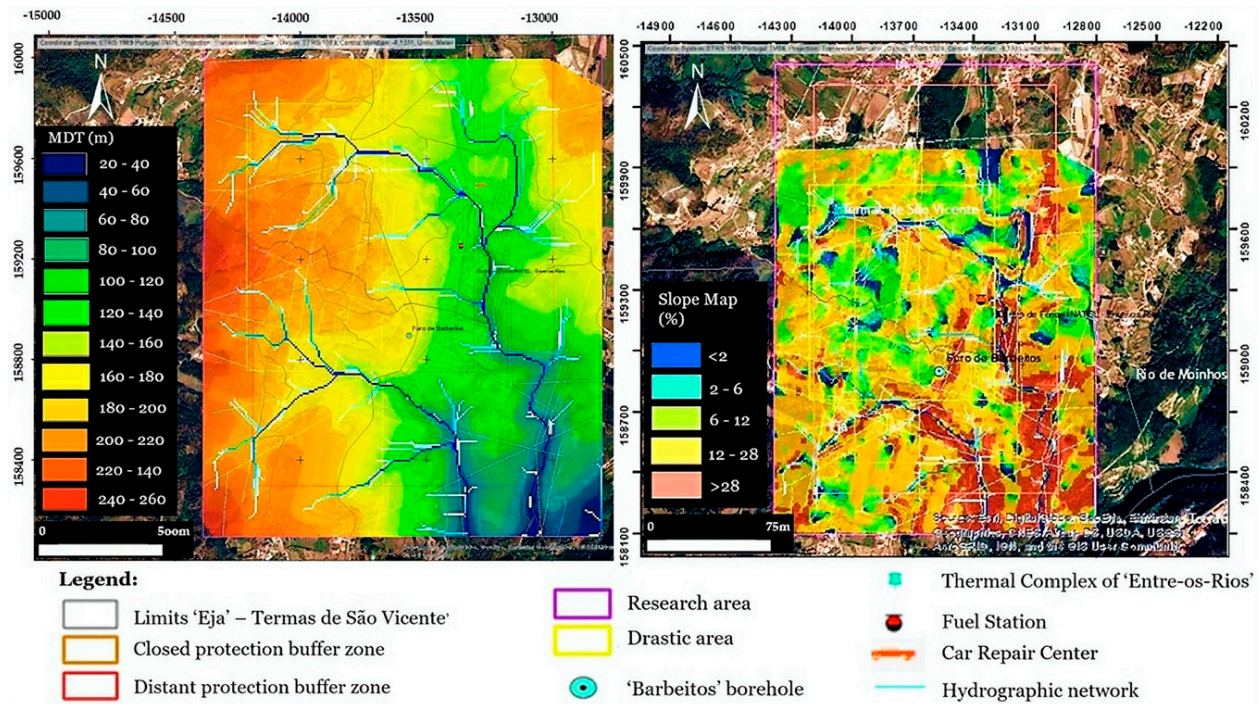


**Figure 3.** Model digital terrain and slope map of the area surrounding the ‘Barbeitos’ borehole.

In terms of the local geology, granitic rocks dominate the research area (Figure 4). The granitic rocks in the research area are part of a band of Variscan granites that extends from ‘Alto Minho’ to ‘Beiras’ from the NW to the SE. The medium-grain porphyroid essentially biotitic two mica monzonitic granite is found over a large region of the map’s NE and has contacts in the SE with the coarse-grained granodiorites and porphyroid granite. Granodiorites and rare biotitic quartzodiorites are present in a lengthy band with a general NW–SE orientation. The contours of this band are quite irregular, and it marks the transition between the previously stated medium-grained granite and the coarse-grained granite. The regional unit is a coarse-grained porphyroid granite with two basically biotitic micas that connect the gap between the two types of granite [3,13,68].

The phylonian rocks can be found all over the place, mostly in granitic formations. Microgranites are particularly abundant in the directions of N–S to NNE–SSW and NE–SW. Sedimentary deposits are scarce, appearing only in the valley bottoms of the ‘Camba’ and ‘Lages’ streams [68]. The hydromineral resources of ‘Entre-os-Rios’ are controlled by tectonic constraints, particularly the deep-crustal fracture systems running N–S to NNE–SSW and ENE–WSW, as well as the regional fracture systems running NW–SE and NE–SW [68].

## 2.2. The Mineral Water

The mineral water seems to occur at the interface of the two types of granite and always in areas of great separation, primarily in the N20°E direction [68] (Figure 5). It seems that the microgranite veins, which are installed throughout the area within granitic masses, influence the emergence of water locally (at least in the ‘Torre’ and ‘Termas de S. Vicente’). Except in the weathered superficial zones of the eruptive rocks and in the existing

colluvium-alluvial patches, formations with secondary permeability due to granite fissures predominate in the study area [64,68].

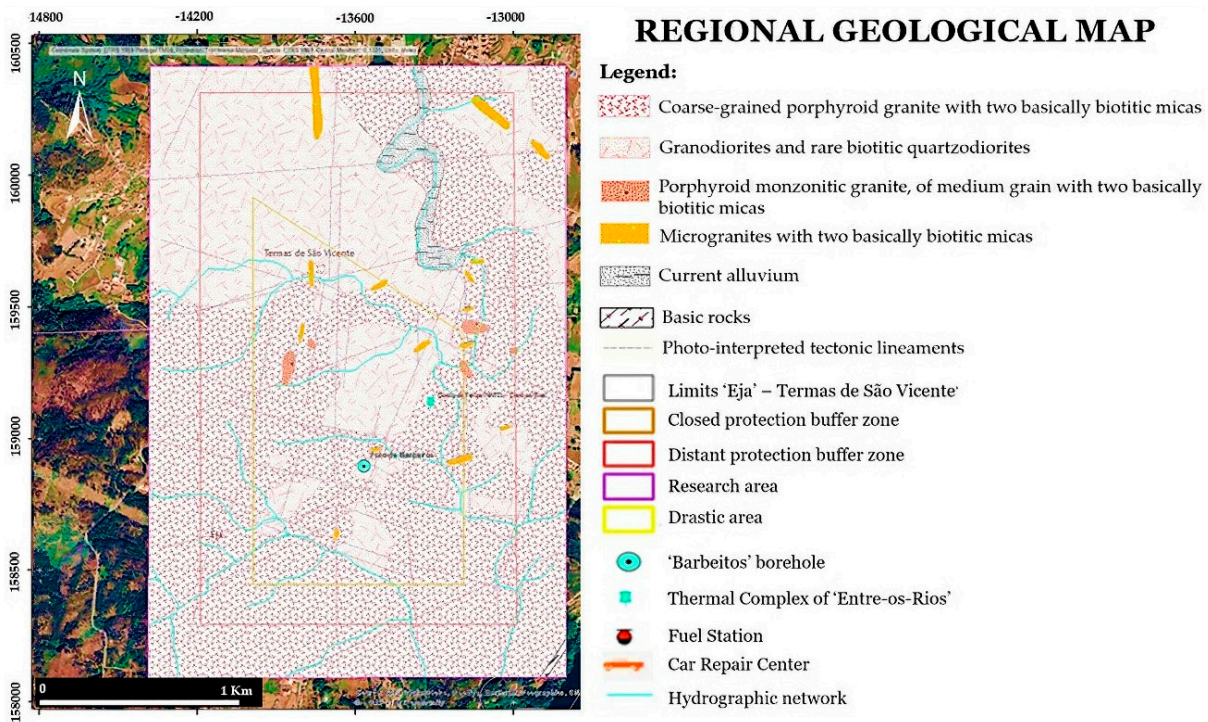


Figure 4. Regional geological outline map of the area surrounding the 'Barbeitos' borehole.

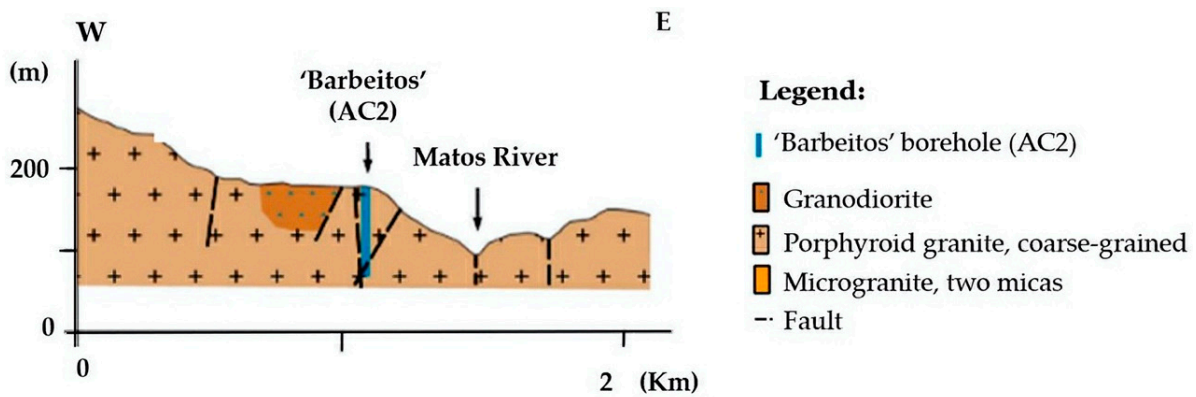


Figure 5. Geological profile of the area surrounding the 'Barbeitos' borehole (adapted from [68]).

In summary, the hydromineral resources of 'Entre-os-Rios' are controlled by: (i) lithology, specifically the geological contact between porphyritic coarse-grained granite and granodiorites, as well as the presence of two-mica microgranite, and (ii) tectonic constraints, primarily the deep-crustal fracture systems running from N–S to NNE–SSW, and ENE–WSW, as well as the regional fracture systems running NW–SE and NE–SW [3,9,68,69]. Granite is the most prevalent lithology, although granites appear in a variety of textures and granularities.

The study area is influenced by an Atlantic mild temperate climate, with annual precipitation ranging from 1300 to 1350 mm, an annual air temperature of 14 °C, annual surface runoff ranging from 600 to 650 mm, annual evapotranspiration ranging from 500 to 550 mm, and annual recharge ranging from 150 to 200 mm [3,9,68]. The water of the thermal springs in 'Entre-os-Rios' is cold, has deep circulation, and has a unique chemistry. The interaction with the silica-rich granite massif results in a pH of approximately 8.8. It is feebly mineralized water, sulphureous, fluoridated, with alkaline and soft reactions [70].

The water from the ‘Barbeitos’ borehole has a low variability in its characteristics over time, allowing for continuous monitoring to infer when contamination emerges in the aquifer [3,9].

The ‘Entre-os-Rios’ hydromineral system is distinguished in the following aquifer systems [68] (Figure 6): (i) at the surface, a highly weathered and decomposed free aquifer that represents a critical role in the recharge of the underlying aquifers; (ii) a free-to-semi-confined aquifer with normal water circulation in weathered zones and in most granite fissure zones (the pH is between 4.1 and 6, the electrical conductivity is less than 150 S/cm, and flow rates are typically less than 0.2 L/s); and (iii) a confined mineral aquifer located in depth near the catchment and conditioned by a zone of structural weakness in depth. The ‘Barbeitos’ borehole located in the granitic rock near contact with granodiorites at a maximum depth of 114 m has an exploitation flow of about 2.5 L/s, a pH of 8.4 to 8.9, and electrical conductivity of 550 to 620 S/cm.

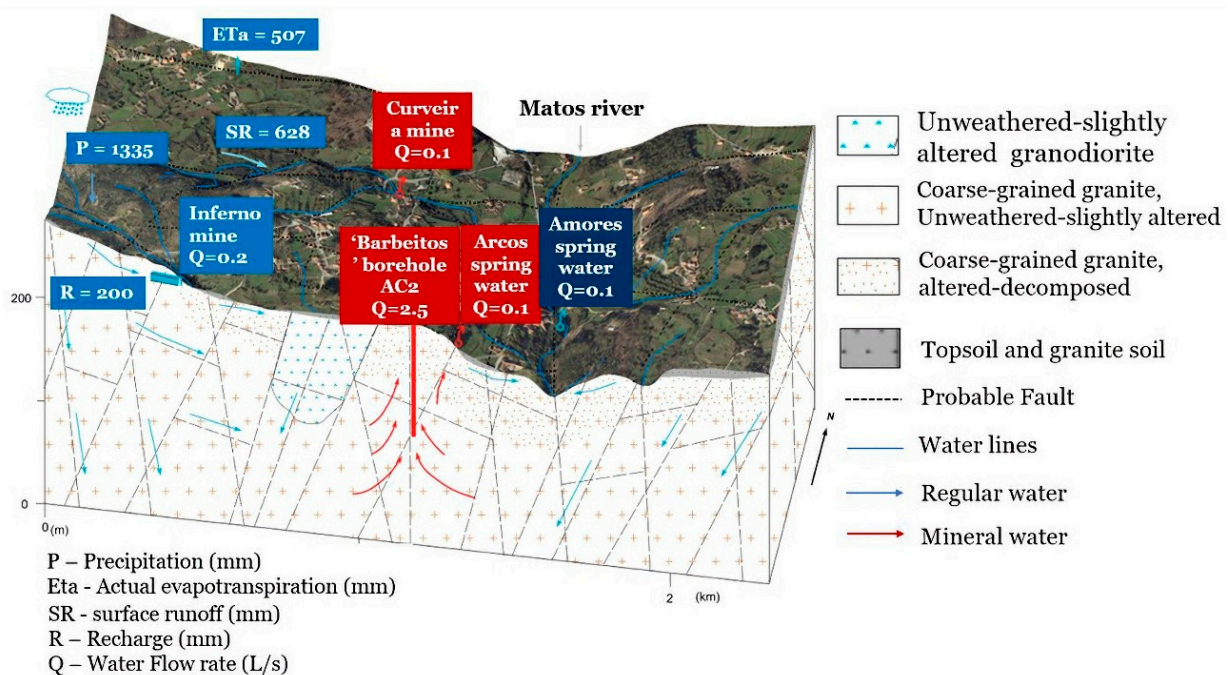


**Figure 6.** Conceptual hydrogeological model of the area surrounding the ‘Barbeitos’ borehole (adapted from [68]).

### 2.3. Development of a Vulnerability Map

The methodology used for creating a vulnerability map for the ‘Barbeitos’ borehole was based on developing thematic maps for all DRASTIC parameters, which is a methodology that was used in the multi-criteria analysis for several environmental problems [55–58]. The DRASTIC index (Equation (1)) was chosen for developing the vulnerability map for the aquifer. This index involves seven parameters [40]: depth to groundwater (D), net recharge (R), material typology of the aquifer (A), soil type (S), topography (T), and the impact of unsaturated (I) and hydraulic conductivity (C). Each parameter is subdivided into representative classes, which are assigned an index (i), ranging from 1 to 10 to correspond with the local hydrogeological characteristics (higher values correspond to greater vulnerability).

$$DI = D_i \times D_p + R_i \times R_p + A_i \times A_p + S_i \times S_p + T_i \times T_p + I_i \times I_p + C_i \times C_p \quad (1)$$

The weights represent the significance of each DRASTIC parameter in relation to the other parameters. The higher the value of the DRASTIC index, the more susceptible that area of the aquifer is to pollution. A thorough understanding of the geology and hydrogeology of the research area is required to define the parameter rating ranges [39,46]. The methodology is presented in Figure 7 as a flow chart.

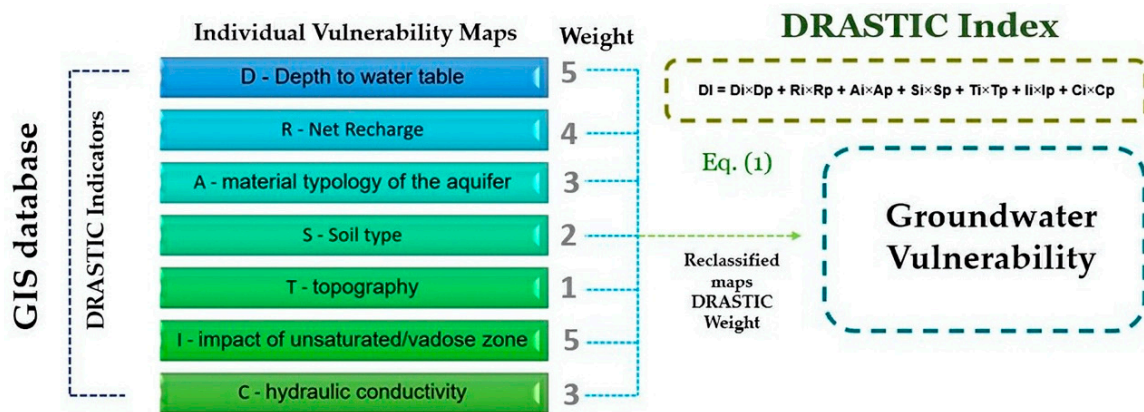


**Figure 7.** Flow chart of the methodology used to develop the groundwater vulnerability map using the DRASTIC model in a GIS.

For processing all maps and data, ESRI’s ArcMap 10.8 software was used, and all information was based on the PT-TM06/ETRS89 Portuguese current official coordinate system. For the construction of the seven thematic maps (one for each variable of the DRASTIC index), a variety of data was collected and processed using ArcGIS tools (Figure 8). The study area was defined and a large range of digital data, tasks, and functions was used. This work involved the confirmation of the information in field visits.

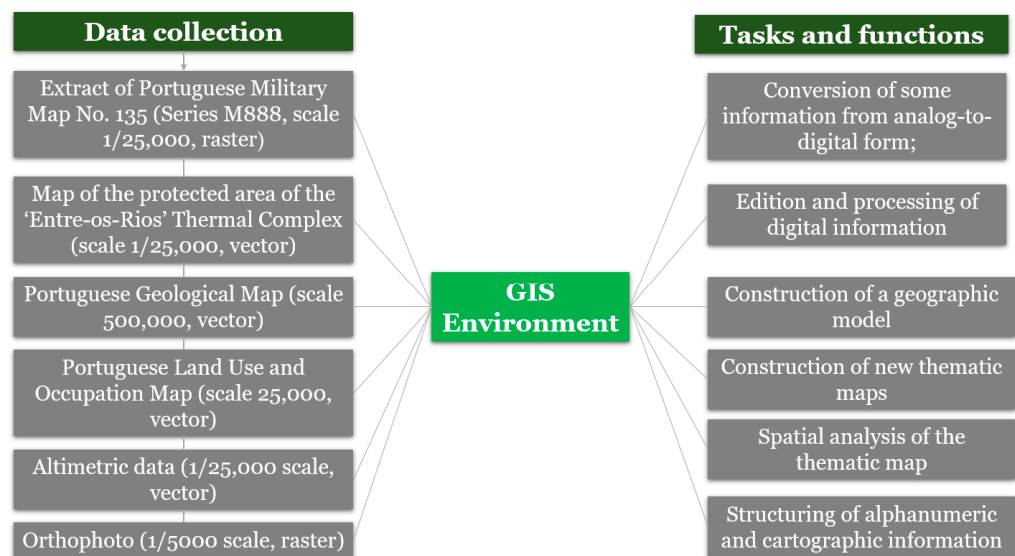


**Figure 8.** Flow chart of the variety of data that was collected and processed using ArcGIS tools and tasks and functions used.

Therefore, the computation procedure was adopted from [56] and involved the overlap of the seven themes through arithmetic operations of maps following Equation (1), as presented in Equation (2).

$$(M_{ij}^k)_{mn} \times W = \sum_{k=1}^{tm} \left( \begin{pmatrix} M_{11}^k & M_{12}^k & \dots & M_{1n}^k \\ M_{21}^k & M_{22}^k & \dots & M_{2n}^k \\ \vdots & \vdots & \dots & \vdots \\ M_{m1}^k & M_{m2}^k & \dots & M_{mn}^k \end{pmatrix} \times W^k \right) \quad (2)$$

where  $(M_{ij}^k)$  is the vector of cell values from each thematic map that is in line  $i$  in row  $j$ ,  $m$  and  $n$  are the dimensions of the thematic grid map,  $k$  is the thematic map,  $tm$  is the number of thematic maps, and  $W$  is the vector of values associated to each cell.

The value of each cell of the final vulnerability map was produced using the arithmetic operation using the value stored in each cell of each thematic map, following Equation (2). Equation (3) was therefore inserted in the Raster Calculator function to calculate the final vulnerability map.

$$(S_{ij})_{mn} = \begin{pmatrix} S_{11} & S_{12} & \cdots & S_{1n} \\ S_{21} & S_{22} & \cdots & S_{2n} \\ \vdots & \vdots & \cdots & \vdots \\ S_{m1} & S_{m2} & \cdots & S_{mn} \end{pmatrix} \quad (3)$$

where  $(S_{ij})$  is the vector of cell values for the suitability map that is in line  $i$  in row  $j$ , and  $m$  and  $n$  are the dimensions of the suitability grid map.

### 3. Results and Discussion

#### 3.1. Thematic Maps for the DRASTIC Index Parameters

The parameter D (depth of groundwater) had an influence on the degree of contact between the percolating contaminant and the subsurface components, as well as the extent and degree of physical and chemical attenuation and degradation [39]. It was calculated using piezometric measurements from a set of 36 georeferenced water points taken in 2008 [68,71]. To interpolate the depth of the aquifer's top, the inverse distance weighted (IDW) method was applied. The IDW interpolation method produced mean values of less than 4 m (Figure 9), corresponding to an index of 9. The areas of greater susceptibility corresponded to zones with shallower aquifer tops, indicating that it was a very sensitive attribute.

The parameter R (net recharge) is the amount of water per unit area of land that percolates through the ground surface and reaches the water table. As a result, the amount of surface cover, the slope of the land surface (Figure 9), soil permeability, and the amount of water that recharges the aquifer all influence it. Contaminant dispersion and dilution are strongly influenced by the amount of water available in the saturated zone, as well as the net recharge. High-recharge-rate regions are more vulnerable than low-recharge-rate areas [40].

The triangulated irregular network (TIN) interpolation model was used, which was converted into a matrix structure, which allowed for creating the slope chart, flow direction, and curvature profile (Figure 10). The curvature profile shows the maximum slope direction and had an impact on the flow acceleration and deceleration, as well as soil erosion and sediment deposition. The union of slope areas less than or equal to 6%, curvature profiles less than or equal to 0, and areas that allow for infiltration formed the map of infiltration potential zones. A recharge of 40 mm/year was assumed using the precipitation values given in [6], resulting in an index value of 1.

The parameter A represents the aquifer's attenuation capacity as a function of the lithology and it is inherently connected to geotechnical parameters [72,73]. Highly permeable lithological formations have higher vulnerability indices because it allows for faster water flow inside the saturated zone [40].

The parameter S evaluates each soil type's capacity to reduce pollution potential. It is essential to analyze the soil properties that influence this potential, such as the thickness, texture, expandability/contractility, and organic matter content [40]. It is considered to be the altered zone's substance, with a thickness of less than 2 m. The thickness of the soil determines the water retention capacity and has a significant impact on the recharge since it aids in the infiltration of precipitation into the ground. For this study, the soil map (Figure 11) was calculated using the values published in [74] for 2018. Forest soil, as well as temporary crops and bushes, are more likely to be affected by pollution.

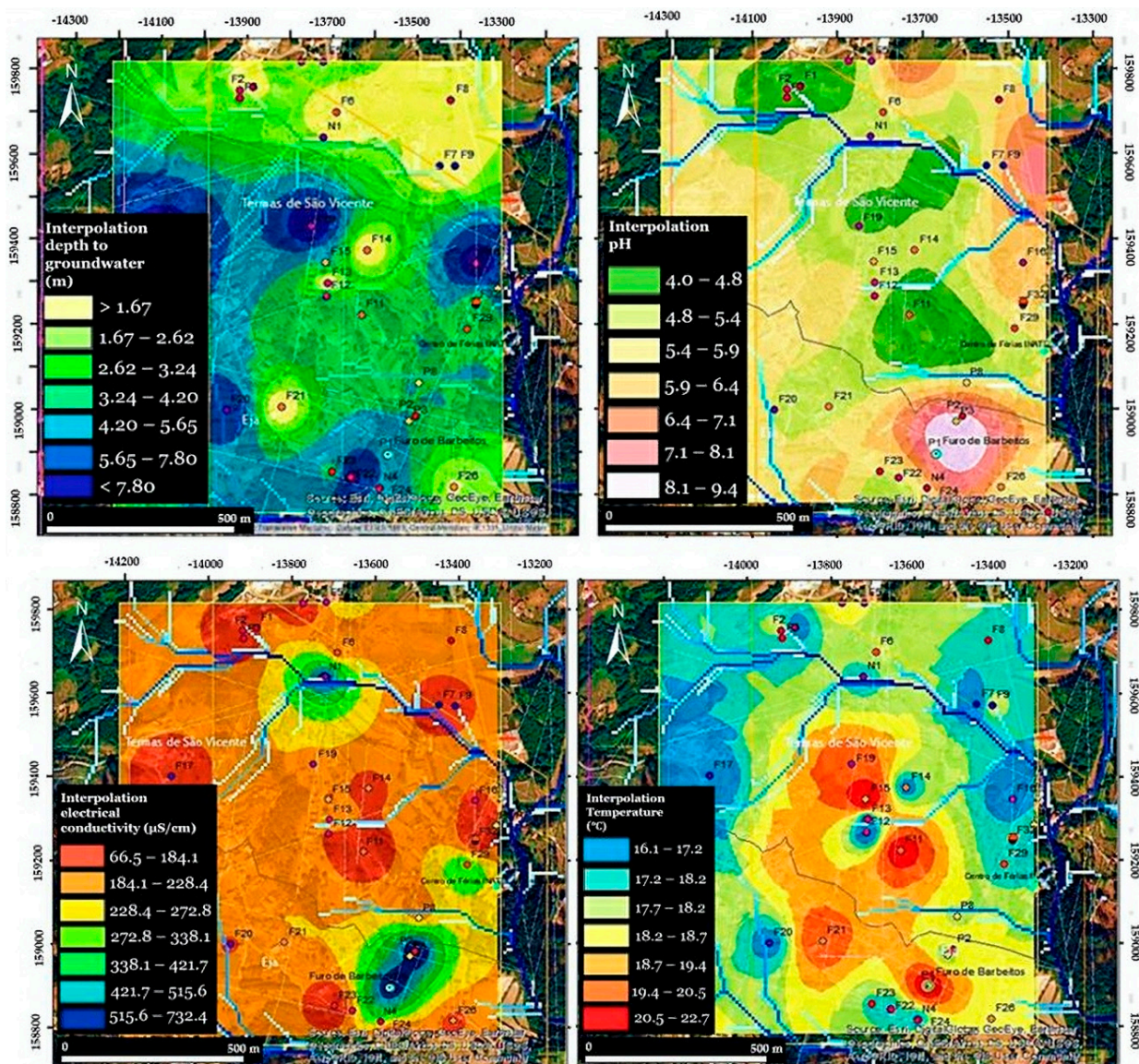


**Figure 9.** Electrical conductivity, pH, temperature, and surface piezometric level interpolation map of the area surrounding the ‘Barbeitos’ borehole.

The ground surface slope and its variation are referred to as the topography. The slope influences the runoff and reveals flat zones where a contaminant can stay on the surface long enough to infiltrate [40]. The parameter T was obtained from the digital terrain model (DTM) and slope map (expressed in percentage). The altimetric data ranges between 20 m and 250 m, with significant slope variations. In low-density areas, where pollutant infiltration is promoted, the vulnerability could be higher.

The parameter I is an important parameter in vulnerability estimation because it influences the residence period of pollutants in the unsaturated zone and, therefore, the probability of attenuation [40].

The parameter C refers to the capacity of the aquifer to transmit water, which, together with the hydraulic gradient, controls the flow of groundwater. Hydraulic conductivity is relative to the quantity and connectivity of open spaces within the aquifer, which can be pores, fractures/cracks, cavities, or discontinuities [40]. High conductivity values are associated with high contamination risks. The parameter was created using a model published in [75] that relates representative values of hydraulic conductivity for various types of rock, as well as values of effective porosity and porosity for certain types of rocks.

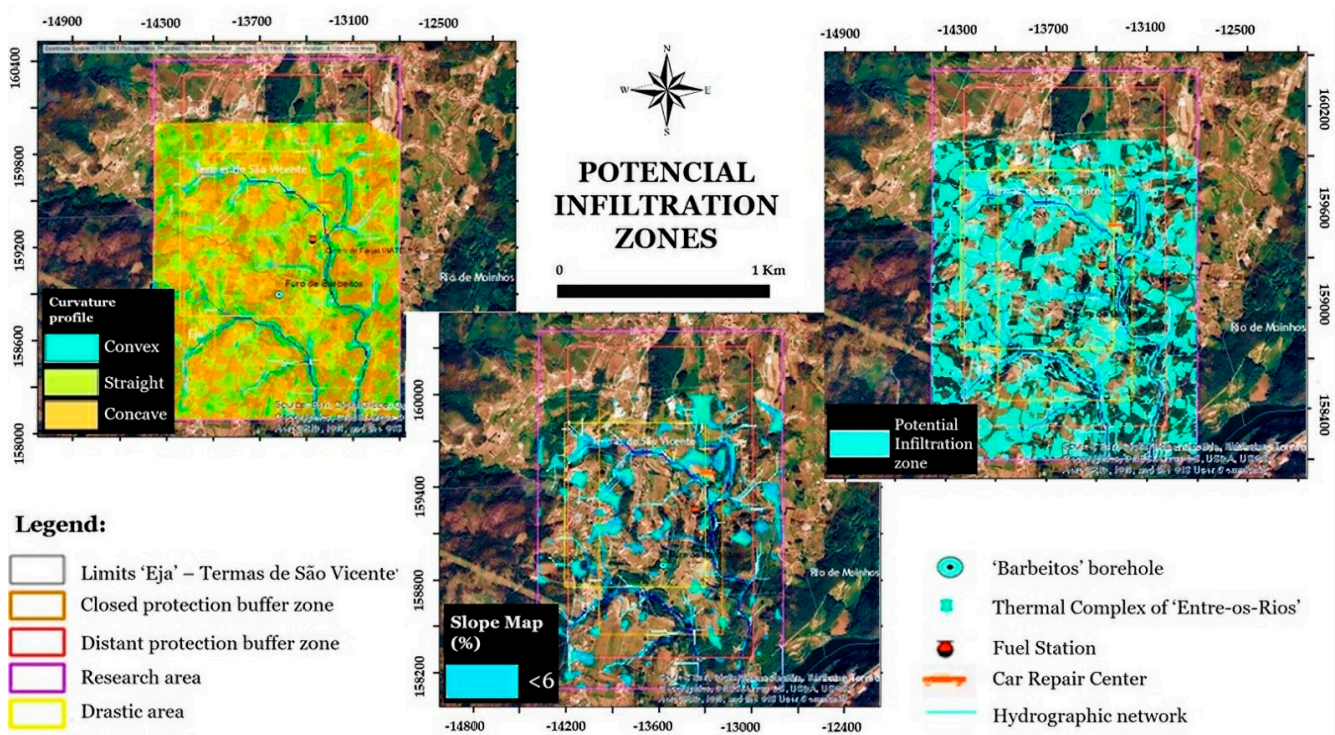


Figure 10. Curvature profile map and infiltration potential areas map of the area surrounding the 'Barbeitos' borehole.

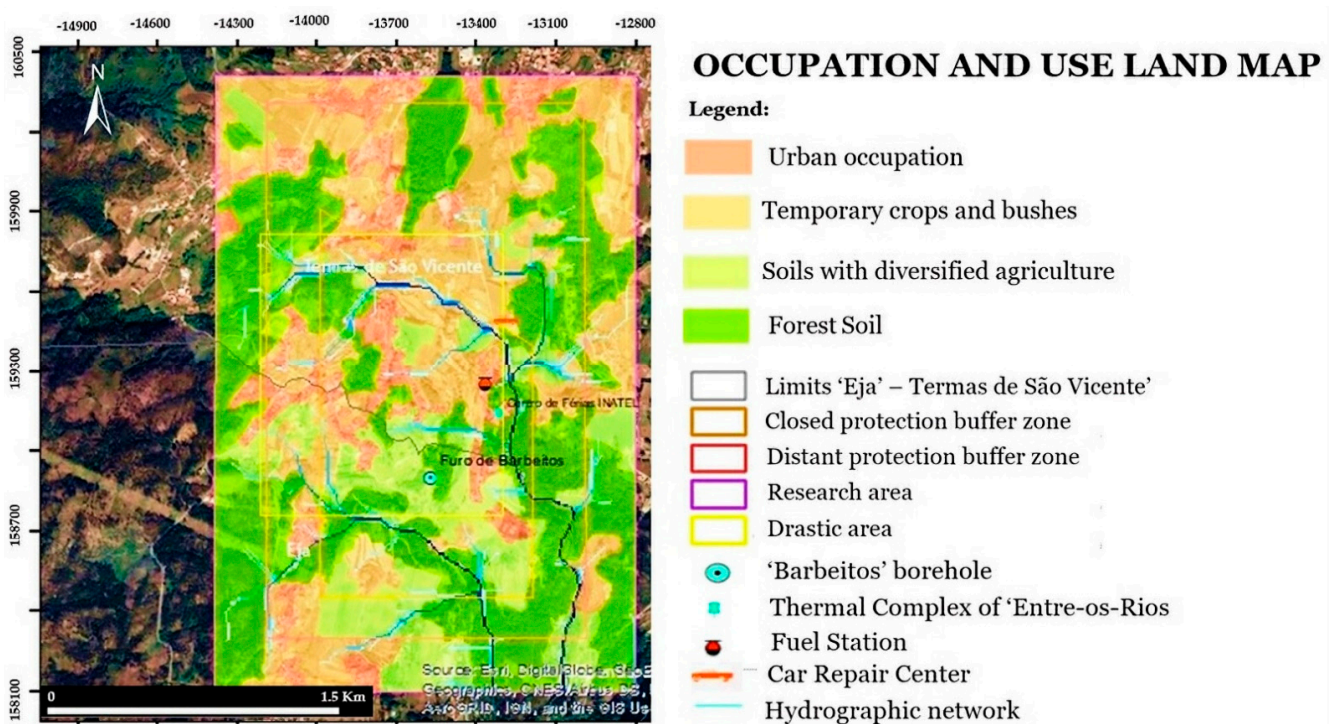


Figure 11. Map of use and land occupation type of the area surrounding the 'Barbeitos' borehole.

The values for quantifying the partial indexes A, I, and C were collected from [76] using a Penafiel map at a 1:500,000 scale. Parameters A and I assumed the prevalence of indexes 2 and 3, which are features of magmatic rocks in the research area. The attribution of greater susceptibility to microgranite outcrops, on the other hand, is cautious because fissural percolation can endanger the aquifer.

### 3.2. Vulnerability Map

Based on new environmental characterization studies, the DRASTIC vulnerability index may sometimes be updated on a regular basis, leading to changes in the final cartography. Table 1 shows the classification of an aquifer's pollution vulnerability based on the LNEC's narrowest classification [77].

**Table 1.** Index value and DRASTIC vulnerability classes (adapted from [40,77]).

General DRASTIC Index	Qualitative Vulnerability
23–79	Insignificant
80–99	Extremely low
100–119	Very low
120–139	Low
140–159	Average
160–179	High
180–199	Very high
200–226	Extremely high

Each of the seven parameters was assigned a weight (p) and an index (i) according to the susceptibility to pollution (Table 2). The DRASTIC vulnerability index map was obtained by overlaying the seven hydrogeological layers in ArcGIS and it used the raster calculator function.

**Table 2.** The weight (p) and index (i) assigned to each of seven parameters used in the DRASTIC vulnerability index modelling of the area surrounding the 'Barbeitos' borehole (adapted from [40]).

Parameters	Classes	Index (i)	Weight (p)
D	<1.50	10	5
	1.50–4.60	9	
	4.60–9.10	7	
	9.10–15.20	5	
R	0–51	1	4
A	Metamorphic/igneous rock	2–5 (3)	3
	Altered metamorphic/igneous rocks	3–5 (4)	
	Sand and ballast	4–9 (8)	
S	Thin or absent	10	2
	Sand	9	
	Loam	5	
	Clay loam	3	
	Non-aggregated and non-expandable clay	1	
T	<2	10	1
	2–6	9	
	6–12	5	
	12–18	3	
	>18	1	
I	Metamorphic/igneous rock	2–8 (4)	5
	Sand and ballast with significant silt and clay percentage	4–8 (6)	
C	<4.10	1	3
	4.10–12.20	2	

The flow in a fissured environment prevails due to the predominance of the granitic rocks present and its fracturing, except in changed surface regions and the current alluvium when the type of flow occurs in a porous material. Since most aquifer recharge occurs in a fissured environment, it is significant to mention that fractures can reach large depths. The aquifer's vulnerability is also determined by the type of filling of these same faults [57].

The vulnerability map for the 'Barbeitos' borehole (Figure 11) was generated by calculating the DRASTIC index (Di) for each 15 × 15 m square using the data in Table 3.

**Table 3.** Values and weights used for calculating the DRASTIC index.

Parameters	Characteristics	(i)	(p)	Range
D	3.9 m (average)	5–10	5	25–50
R	Deep recharge	0–1	4	0–4
A	Permeability	2–7	3	6–21
S	Change areas (<2 m)	1–6	2	2–12
T	Slope map	1–10	1	1–10
I	Unsaturated zone lithology	2–6	5	10–30
C	Capacity to transmit water	1–2	3	3–6
DRASTIC index (DI)				47–127

The risk includes the vulnerability and presence of sources of pollution, and the environmental context in the study area where the catchment was located is reasonable. The DRASTIC index's values ranged from 47 to 127 points, ranging from insignificant to moderate, with an average pollution vulnerability of 79 points for 'normal' pollutants.

The intrinsic vulnerability in the study area was obtained as a result of the weighted sum of the various maps related to each of the attributes according to the DRASTIC methodology (Figure 12).

Alluvium-covered land is vulnerable to moderate contamination; however, it is located far from the catchment. Because of the conditions to which they are subjected, the areas occupied by microgranites and where meteoric water infiltrates, along with preferential recharge sectors that are hydraulically linked to deep fracturing, represent a moderate vulnerability. On the other hand, areas of minimal risk could correspond to locations where the granitic massif has not been significantly altered. The study location is in a sloping terrain bounded by granitic outcrops, indicating a low vulnerability to contamination. However, as previously stated, fracturing can transport pollutants to great depths and/or distances.

Mineral water is of meteoric origin, with a long time of permanence in the deep system, classifying these waters among the slowest in the set of sulphur waters in the country. The pH value is around 8.8, meaning it is of basic character, which results from the interaction with the granitic massif that is rich in silica. The temperature has an average value of 20.5 °C, which belongs to the class of hypothermal waters.

Using several approaches to defining protection perimeter buffer zones (Figure 13) allows for the long-term preservation of the quality of the hydromineral resource. For the immediate buffer zone, a radius of 50 m is proposed, with the center of the circle representing the mineral water catchment. According to [39], this radius is justified by current legislation, as well as the fact that it is an aquifer system whose lithological foundation is made up of igneous rocks that differ in their alteration from highly altered to little altered. It has a total area of 0.785 ha and must be completely closed to any intrusion and always kept clean.

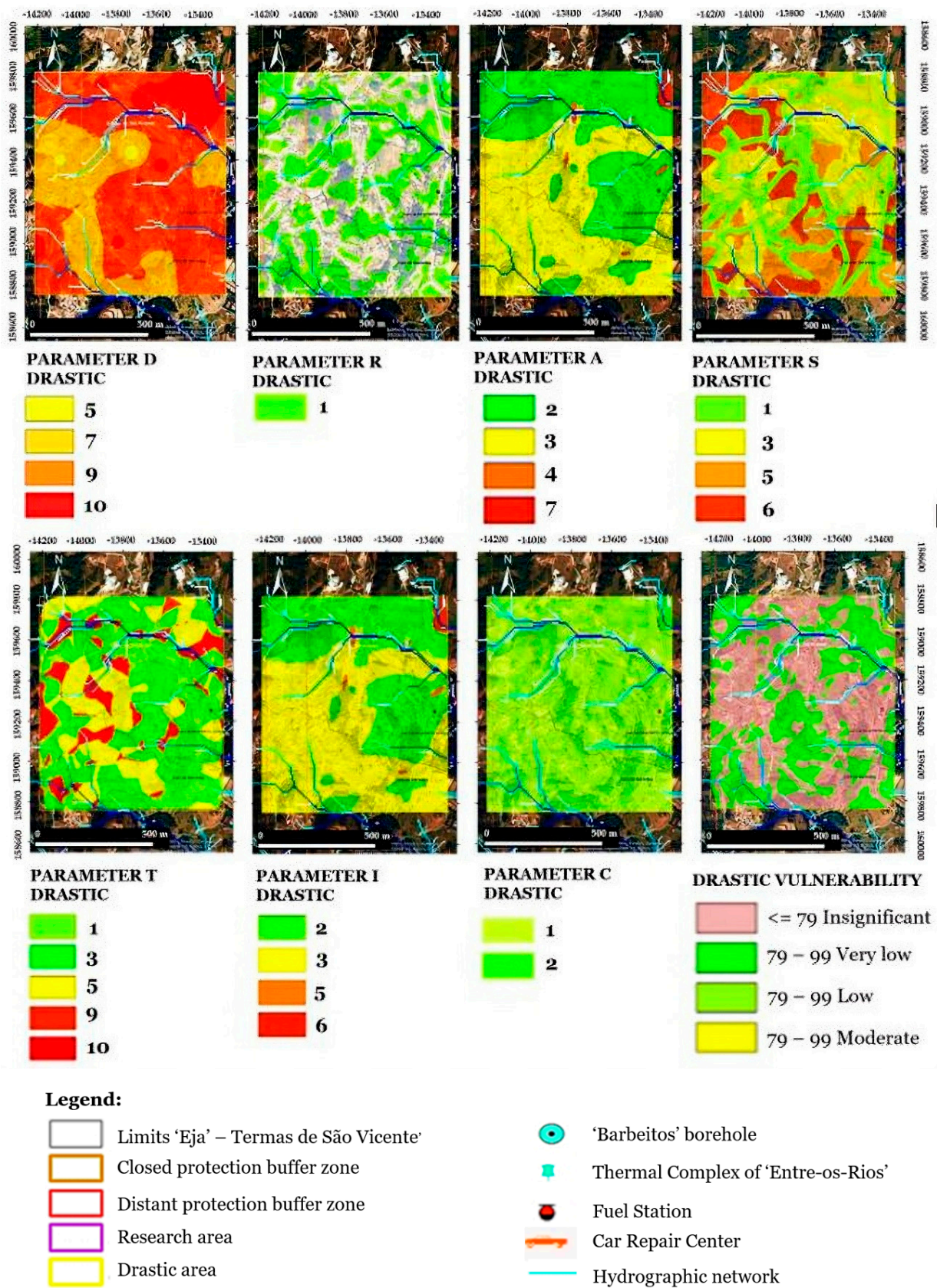
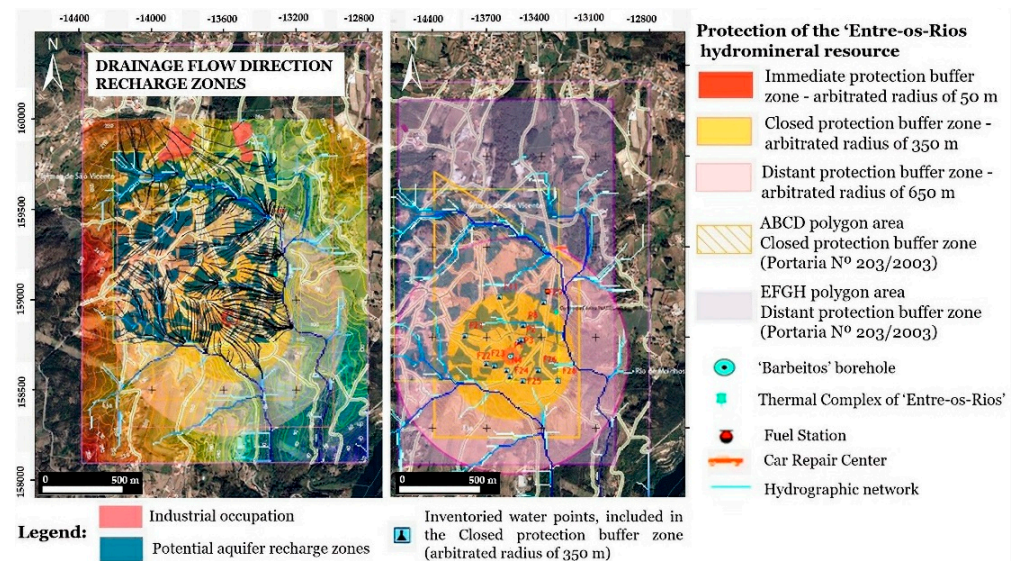


Figure 12. Map of parameters (D, R, A, S, T, I, C) and map of vulnerability to pollution of the 'Entre-os-Rios' aquifer.



**Figure 13.** Map of the final considerations of the 'Barbeitos' borehole protection zones.

The near buffer zone is defined by geological-structural, hydrogeological, and pollution vulnerability parameters. It coincides with the concession area, occupying an area of 96.6 ha. Its purpose is to protect against direct interference in the local emergency mechanism, particularly N-oriented fracturing and potentially ENE and NNE fracturing. The limits of the distant protection buffer zone, which covers 241.8 ha, were established to include preferred recharge sectors that are hydraulically related to deep fractures. The favourable circulation of the aqueous system under study is related to the N–S and NE–SW directions. The purpose of this area is to prevent contamination zones from developing, preventing further surface runoff and subsurface pollution. It was not enough to define areas that are off-limits to certain uses. These areas must also be monitored for contaminants that may be carried in the subsurface flow current. Although it is difficult to limit all activities while maintaining perfect aquifer preservation, it is critical that the activities be totally compatible with the preservation of the hydromineral resource within the legislatively established limits. In this context, GIS has great potential as a tool for georeferenced data processing and analysis and it can be employed to develop long-term management strategies. A GIS has considerable potential in this context as a tool for georeferenced data processing and analysis and it can be employed to develop long-term management strategies. Groundwater vulnerability mapping and hydrogeological cartography are excellent tools for aiding in the description, assessment, modelling, and communication of groundwater resources.

#### 4. Conclusions

This work allowed for the determination of the intrinsic vulnerability of groundwater in the surroundings of the 'Barbeitos' borehole through the calculation of a pollution vulnerability map, by applying the DRASTIC index. The vulnerability map shows that the protection perimeter buffer zone had a low vulnerability to pollution, which was partly related to the geological characteristics of the region, and since the microgranites were quite distant, this tended to prevent polluting compounds from infiltrating.

Even though the closed and distant protection buffer zones defined for the 'Barbeitos' are oversized, both in the direction of flow and perpendicular to it, it is important to consider the heterogeneity of the underground environment in the study area, the possibility of preferential flow through high fracturing density of the fault zones surrounding the catchment, and the uncertainty associated with method application due to the indeterminacy of some hydraulic parameters. It is crucial to note that the areas are adjusted to the occupation and use of the land of the region and that the gas station caused a fuel spill of

more than 4000 L, which exceeded the area of this land and infiltrated adjacent land under the concession. Although the company responsible removed approximately 380 tonnes of polluted soil in 2002, it should be noted that the compaction of the replacement material may have locally affected the hydraulic parameters of the aquifer. The entire area of the increased protective perimeter of the 'Entre-os-Rios' hydromineral concession needs to be monitored in terms of groundwater quality, particularly in the boreholes nearest to the catchment. Pesticides and fertilizers could contaminate the area near the 'Barbeitos' well because the area is widely used for agriculture. It is crucial to identify possible residences where there is a lack of basic sanitation in the absence of a septic tank since the infiltration of these tributaries at higher levels could be a source of diffuse pollution. According to LNEC (2008) [71], this scenario is represented in a hole just 100 m north of the concession that is bacteriologically unsafe for human consumption. The same report revealed the presence of hydrocarbons in the holes near the fuel pump and downstream of it, which reaches the Barbeitos well in very low proportions. However, active natural attenuation processes, such as anaerobic biodegradation reactions, may occur.

In the assessment of groundwater's inherent vulnerability to pollution, the DRASTIC model produced acceptable results. However, in order to acquire more precise outcomes, the original model must be adjusted and modified over time. The density of lineaments, land usage, and land cover are significant terrain parameters that influence the flow and infiltration of contaminants.

The presence of this type of water (predominantly sulphur waters) is usually linked to unique hydrogeological conditions, which requires the adjustment of territorial planning strategies for its preservation, considering the heritage, cultural, and scientific qualities to which it is linked.

**Author Contributions:** Conceptualization, V.G. and V.C.; methodology, V.G., A.A., P.G.A. and V.C.; validation, P.G.A. and V.C.; formal analysis, V.G., A.A., P.G.A. and V.C.; data curation, V.G., A.A., P.G.A. and V.C.; writing—original draft preparation, V.G.; writing—review and editing, A.A. and P.G.A.; supervision, V.C. All authors have read and agreed to the published version of the manuscript.

**Funding:** This research received no external funding.

**Acknowledgments:** The authors are grateful to the Foundation for Science and Technology (FCT, Portugal) for supporting the research through the projects UIDB/00195/2020 (FibEnTech) and UIDB/04035/2020 (GeoBioTec).

**Conflicts of Interest:** The authors declare no conflict of interest.

## References

1. Carvalho, J. Mineral water exploration and exploitation at the Portuguese Hercynian Massif. *Environ. Geol.* **1996**, *27*, 252–258. [[CrossRef](#)]
2. Juncosa, R.; Mejjide-Failde, R.; Delgado, J. Therapeutic characteristics of Galician mineral and thermal waters (NW-Spain) ascribed to their local/regional geological setting. *Sustain. Water Resour. Manag.* **2019**, *5*, 83–99. [[CrossRef](#)]
3. Afonso, M.J.; Chaminé, H.I. Environmental hydrogeochemistry assessment as a tool for sustainable hydromineral resources management (Entre-os-Rios thermal baths, NW Portugal). *Sustain. Water Resour. Manag.* **2019**, *5*, 147–159. [[CrossRef](#)]
4. Ferreira Gomes, L.; Antunes, I.; Albuquerque, M.; Santos Silva, A. New Thermal 823 Mineral Water from Águas (Penamacor, Central Portugal): Hydrogeochemistry and Therapeutic Indications. In Proceedings of the IOP Conference Series: Earth and Environmental Science, Prague, Czech Republic, 3–7 September 2018; Volume 221. [[CrossRef](#)]
5. Albu, X.; Banks, X.; Nash, X. *Mineral and Thermal Groundwater Resources*; Chapman & Hall: London, UK, 1997.
6. LaMoreaux, P.E.; Tanner, J.T. *Springs and Bottled Waters of the World: Ancient History, Source, Occurrence, Quality and Use*; Springer: Berlin, Germany, 2001.
7. Marques, J.M.; Carreira, P.M.; Neves, O.; Espinha Marques, J.; Teixeira, J. Revision of the hydrogeological conceptual models of two Portuguese thermomineral water systems: Similarities and differences. *Sustain. Water Resour. Manag.* **2019**, *5*, 117–133. [[CrossRef](#)]
8. Freeze, R.A.; Cherry, J.A. *Groundwater*; Prentice-Hall: Englewood Cliffs, NJ, USA, 1979.
9. Marques, J.M.; Matos, C.; Carreira, P.M. Isotopes and geochemistry to assess shallow/thermal groundwater interaction in a karst/fissured-porous environment (Portugal): A review and reinterpretation. *Sustain. Water Resour. Manag.* **2017**, *5*, 1525–1536. [[CrossRef](#)]

10. Cantista, P. O Termalismo em Portugal. *An. Hidrol. Med.* **2008**, *3*, 79–107. Available online: <http://www.journals4free.com/link.jsp?l=17647061> (accessed on 15 January 2022). (In Portuguese)
11. Decree Law n.º 156/98, June 6th. Lays out the Guidelines for Recognizing Natural Mineral Waters, as Well as the Traits and Requirements That Must Be Met When Treating, Labelling, and Marketing Natural Mineral Waters and Spring Waters. *Diário da República* n.º 131/1998, Série I-A de 1998-06-06, Páginas 2593–2599. Available online: <https://dre.pt/dre/detalhe/decreto-lei/156-1998-473321> (accessed on 15 January 2022).
12. Lepierre, C. *Chimie et Physico-Chimie des Eaux (Le Portugal Hydrologique et Climatique)*, 1st ed.; Monography; Industria Graficas: Lisboa, Portugal, 1930. (In French)
13. Afonso, M.J.; Ferreira, M.R.; Teixeira, J.; Chaminé, H.I. The sulphurous mineral waters of Entre-os-Rios (NW Portugal): A hydro-geochemical assessment. In Proceedings of the 1st International Congress on Water Healing Spa and Quality of Life/I Congreso Internacional del Auga, Termalismo y Calidad de Vida 2016, Ourense, Spain, 23–24 September 2015; Failde, J.M., Formella, A., Fraiz, J.Á., Gómez-Gesteira, M., Pérez, F., Vázquez, V.R., Eds.; pp. 169–174.
14. Acciaiuoli, L.M.C. Le Portugal hydrominéral. In *Direction Générale des Mines et des Services Géologiques*; DGMSG: Lisbon, Portugal, 1952; Volume 2.
15. Croutier, A.L. *Taking the Waters: Spirit, Art, Sensuality*, 1st ed.; Abbeville Press: New York, NY, USA, 1992; Volume 7.
16. Jackson, R. Waters, and spas in the classical world. *Med. History* **1990**, *34*, 1–13. [[CrossRef](#)]
17. Giampaoli, S.; Romano Spica, V. Health and safety in recreational waters. *Bull. World Health Organ.* **2014**, *92*, 79. [[CrossRef](#)]
18. Van Tubergen, A.; Van der Linden, S.A. Brief History of Spa Therapy. *Ann. Rheum. Dis.* **2002**, *61*, 273–275. [[CrossRef](#)]
19. Routh, H.B.; Bhowmik, K.R.; Parish, L.C.; Witkowski, J.A. Balneology, mineral water, and spas in historical perspective. *Clin. Dermatol.* **1996**, *14*, 551–554. [[CrossRef](#)]
20. Valeriani, F.; Margarucci, L.M.; Spica, V.R. Recreational Use of Spa Thermal Waters: Criticisms and Perspectives for Innovative Treatments. *Int. J. Environ. Res. Public Health* **2018**, *15*, 2675. [[CrossRef](#)] [[PubMed](#)]
21. Frosh, W.A. Taking the waters—Springs, wells, and spas. *FASEB J.* **2007**, *21*, 1948–1950. [[CrossRef](#)] [[PubMed](#)]
22. Frost, G.J. The spa as a model of an optimal healing environment. *J. Altern. Complement. Med.* **2004**, *10*, 85–92. [[CrossRef](#)]
23. Morer, C.; Roques, C.F.; Françon, A.; Forestier, R.; Maraver, F. The role of mineral elements and other chemical compounds used in balneology: Data from double-blind randomized clinical trials. *Int. J. Biometeorol.* **2017**, *61*, 2159–2173. [[CrossRef](#)]
24. Araujo, A.R.T.S.; Sarraguça, M.C.; Ribeiro, M.P.; Coutinho, P. Physicochemical fingerprinting of thermal waters of Beira Interior region of Portugal. *Environ. Geochem. Health* **2017**, *39*, 483–496. [[CrossRef](#)]
25. Matsumoto, S. Evaluation of the Role of Balneotherapy in Rehabilitation Medicine. *J. Nippon. Med. Sch.* **2018**, *85*, 196–203. [[CrossRef](#)]
26. Petracchia, L.; Liberati, G.; Masciullo, S.G.; Grassi, M.; Fraioli, A. Water, Mineral Waters and Health. *Clin. Nutr.* **2006**, *25*, 377–385. [[CrossRef](#)]
27. Mavridou, A.; Pappa, O.; Papatitze, O.; Blougoura, A.; Drossos, P. An overview of pool and spa regulations in Mediterranean countries with a focus on the tourist industry. *J. Water Health* **2014**, *12*, 359–371. [[CrossRef](#)]
28. WWAP. *The United Nations World Water Development Report: Groundwater: Making the Invisible Visible*; UNESCO: Paris, France, 2022. [[CrossRef](#)]
29. Tang, F.H.M.; Lenzen, M.; McBratney, A.; Maggi, F. Risk of pesticide pollution at the global scale. *Nat. Geosci.* **2021**, *14*, 206–210. [[CrossRef](#)]
30. Sharma, A.; Kumar, V.; Shahzad, B.; Tanveer, M.; Singh Sidhu, G.P.; Handa, N.; Kohli, S.K.; Yadav, P.; Bali, A.S.; Parihar, R.D.; et al. Worldwide pesticide usage and its impacts on ecosystem. *Appl. Sci.* **2019**, *1*, 1446. [[CrossRef](#)]
31. Silva, F.; Albuquerque, A.; Cavaleiro, V.; Scalize, P. Removal of Cr, Cu and Zn from liquid effluents using the fine component of granitic residual soils. *Open Eng.* **2018**, *8*, 417–425. [[CrossRef](#)]
32. Belizário, P.; Scalize, P.; Albuquerque, A. Heavy metal removal in a detention basin for road runoff. *Open Eng.* **2016**, *6*, 412–417. [[CrossRef](#)]
33. Silva, F.; Scalize, P.; Crunivel, K.; Albuquerque, A. Caracterização de solos residuais para infiltração de efluente de estação de tratamento de esgoto. *Rev. Eng. Sanitária E Ambient.* **2017**, *22*, 95–102. [[CrossRef](#)]
34. Borevsky, B.; Yazvin, L.; Margat, L. Importance of groundwater for water supply. In *Groundwater Resources of the World and Their Use*; IHP-VI, Series on Groundwater; Zektser, I.S., Everett, L.G., Eds.; UNESCO: Paris, France, 2004; pp. 20–24.
35. Foster, S.S.D.; Chilton, P.J. Groundwater: The processes and global significance of aquifer degradation. *Philos. Trans. R Soc. Lond. B* **2003**, *358*, 1957–1972. [[CrossRef](#)] [[PubMed](#)]
36. Duarte, L.; Teodoro, A.C.; Gonçalves, J.A.; Guerner Dias, A.J.; Espinha Marques, J. A dynamic map application for the assessment of groundwater vulnerability to pollution. *Environ. Earth Sci.* **2015**, *74*, 2315–2327. [[CrossRef](#)]
37. Fang, Z.; Liu, Z.; Zhao, S.; Ma, Y.; Li, X.; Gao, H. Assessment of Groundwater Contamination Risk in Oilfield Drilling Sites Based on Groundwater Vulnerability, Pollution Source Hazard, and Groundwater Value Function in Yitong County. *Water* **2022**, *14*, 628. [[CrossRef](#)]
38. Živanović, V.; Atanacković, N.; Stojadinović, S. Vulnerability Assessment as a Basis for Sanitary Zone Delineation of Karst Groundwater Sources—Blederija Spring Case Study. *Water* **2021**, *13*, 2775. [[CrossRef](#)]

39. Decree Law n.º 382/99 de 22 de Setembro, Establishes Protection Perimeters for Groundwater Abstraction Intended for Public Supply. Portuguese Law, Diário da República n.º 222, I Série, 1999, Lisboa, Portugal. Available online: <https://data.dre.pt/eli/dec-lei/382/1999/09/22/p/dre/pt/html> (accessed on 20 January 2022).
40. Aller, L.; Lehr, J.H.; Petty, R.; Bennet, T. *DRASTIC: A Standardized System to Evaluate Groundwater Pollution Potential Using Hydrogeologic Settings*; National Water Well Association: Worthington, OH, USA, 1987.
41. Foster, S.S.D. Fundamental concepts in aquifer vulnerability, pollution risk and protection strategy. In *Vulnerability of Soil and Groundwater to Pollutants*; Proceedings and Information no. 38; Van Duijvenbooden, W., van Waegeningh, H.G., Eds.; TNO Committee on Hydrological Research: The Hague, The Netherlands, 1987; pp. 69–86.
42. NAP (National Academies Press). *Groundwater Vulnerability Assessment-Contamination Potential under Conditions of Uncertainty*; NAP: Washington, DC, USA, 1993; p. 189. [\[CrossRef\]](#)
43. Medici, G.; Engdahl, N.B.; Langman, J.B. A basin-scale groundwater flow model of the columbia plateau regional aquifer system in the palouse (USA): Insights for aquifer vulnerability assessment. *Int. J. Environ. Res.* **2021**, *15*, 299–312. [\[CrossRef\]](#)
44. Ducci, D.; Sellerino, M. Vulnerability mapping of groundwater contamination based on 3D lithostratigraphical models of porous aquifers. *Sci. Total Environ.* **2013**, *447*, 315–322. [\[CrossRef\]](#)
45. Jang, W.S.; Engel, B.; Harbor, J.; Theller, L. Aquifer Vulnerability Assessment for Sustainable Groundwater Management Using DRASTIC. *Water* **2017**, *9*, 792. [\[CrossRef\]](#)
46. Al-Zabet, T. Evaluation of aquifer vulnerability to contamination potential using the DRASTIC method. *Environ. Geol.* **2002**, *43*, 203–208. [\[CrossRef\]](#)
47. Shirazi, S.M.; Imran, H.M.; Shatirah, A. GIS-Based DRASTIC method for groundwater vulnerability assessment: A review. *J. Risk Res.* **2012**, *15*, 991–1011. [\[CrossRef\]](#)
48. Dixon, B. Groundwater vulnerability mapping: A GIS and fuzzy rule based integrated tool. *Appl. Geogr.* **2005**, *25*, 327–347. [\[CrossRef\]](#)
49. Machiwal, D.; Jha, M.K.; Singh, V.P.; Mohan, C. Assessment and mapping of groundwater vulnerability to pollution: Current status and challenges. *Earth Sci. Rev.* **2018**, *185*, 901–927. [\[CrossRef\]](#)
50. Rossetto, R.; Sabbatini, T.; Silvestri, N. Assessing Specific Vulnerability of Shallow Aquifers to Pesticide Using GIS Tools. Data Needs and Reliability of Index-Overlay Methods: An Application to the San Giuliano Terme Agricultural Area (Pisa, Italy). *Agronomy* **2020**, *10*, 985. [\[CrossRef\]](#)
51. Paralta, E.; Frances, A.; Ribeiro, L. Avaliação da vulnerabilidade do sistema aquífero dos Grabos de Beja e análise crítica das redes de monitorização no contexto da directiva da água. In Proceedings of the VII Simpósio de Hidráulica e Recursos Hídricos dos Países de Língua Portuguesa 2005 (7º SILUSBA), Évora, Portugal, 30 May–2 June 2005. (In Portuguese).
52. Wang, J.; He, J.; Chen, H. Assessment of groundwater contamination risk using hazard quantification, a modified DRASTIC model, and groundwater value, Beijing Plain, China. *Sci. Total Environ.* **2012**, *432*, 216–226. [\[CrossRef\]](#)
53. Jenifer, M.; Jha, M. A Novel GIS-Based Modeling Approach for Evaluating Aquifer Susceptibility to Anthropogenic Contamination. *Sustainability* **2022**, *14*, 4538. [\[CrossRef\]](#)
54. Baalousha, H.; Tawabini, B.; Seers, T. Fuzzy or Non-Fuzzy? A Comparison between Fuzzy Logic-Based Vulnerability Mapping and DRASTIC Approach Using a Numerical Model. A Case Study from Qatar. *Water* **2021**, *13*, 1288. [\[CrossRef\]](#)
55. Teixeira, J.; Chaminé, H.I.; Carvalho, J.M.; Pérez-Alberti, A.; Rocha, F. Hydrogeomorphological mapping as a tool in groundwater exploration. *J. Maps* **2013**, *9*, 263–273. [\[CrossRef\]](#)
56. Pedrero, F.; Albuquerque, A.; Marecos do Monte, H.; Cavaleiro, V.; Alarcón, J. Application of GIS-based multi-criteria analysis for site selection of aquifer recharge with reclaimed water. *Resour. Conserv. Recycl.* **2011**, *56*, 105–116. [\[CrossRef\]](#)
57. Ribeiro, P.; Albuquerque, A.; Quinta-Nova, L.; Cavaleiro, V. Recycling of pulp mill sludge to improve soil fertility using GIS tools. *Resour. Conserv. Recycl.* **2010**, *54*, 1303–1311. [\[CrossRef\]](#)
58. Albuquerque, A.; Scalize, P.; Ferreira, N.; Silva, F. Multi-criteria analysis for site selection for the reuse of reclaimed water and biosolids. *Ambiente & Água—An Interdisciplinary. J. Appl. Sci.* **2015**, *10*, 22–34. [\[CrossRef\]](#)
59. Teixeira, J.; Chaminé, H.; Espinha Marques, J.; Carvalho, J.; Pereira, A.; Carvalho, M.; Fonseca, P.; Pérez-Alberti, A.; Rocha, F. A comprehensive analysis of groundwater resources using GIS and multicriteria tools (Caldas da Cavaca, Central Portugal): Environmental issues. *Environ. Earth Sci.* **2015**, *73*, 2699–2715. [\[CrossRef\]](#)
60. Teixeira, J.; Chaminé, H.I.; Espinha Marques, J.; Gomes, A.; Carvalho, J.M.; Pérez-Alberti, A.; Rocha, F. *Integrated Approach of Hydrogeomorphology and GIS Mapping to the Evaluation of Groundwater Resources: An Example from the Hydromineral System of Caldas da Cavaca, NW Portugal*; Paliwal, B.S., Ed.; Global Groundwater Resources and Management, Scientific Publishers: Jodhpur, India, 2010; pp. 227–249. Available online: <http://hdl.handle.net/10216/22208> (accessed on 25 January 2022).
61. Chaminé, H.; Carvalho, J.; Teixeira, J.; Freitas, L. Role of hydrogeological mapping in groundwater practice: Back to basics. *Eur. Geol. J.* **2015**, *40*, 34–42. Available online: <https://hdl.handle.net/10216/81056> (accessed on 25 January 2022).
62. Mejuto, M.; Castaño, S.; Vela, A. Utilidad de las Técnicas de Observación de la Tierra a Lá Elaboración de Mapas de Vulnerabilidad y Riesgo de Contaminación de Aguas Subterráneas. In Proceedings of the VIII Congreso Nacional de Teledetección 1999, Albacete, Espanha, 22–24 September 1999. (In Spanish).
63. Xavier, J.; Gagliardi, S.; Vidal, H.; Montano, M.; Lucena, L.R.F. Evaluación de la vulnerabilidad a la contaminación del acuífero Mercedes en el área metropolitana de la Ciudad de Paysandú—Comparación de los Métodos GOD y DRASTIC. *Rev. Lat.*

- Am. Hidrogeol.* **2004**, *4*, 5–46. Available online: <http://ceregas.org/files/Repositorio%20documentos%20agua%20subterranea/Documentos%20del%20excel/55.pdf> (accessed on 30 January 2022). (In Spanish).
64. Carvalho, P.; Cavaleiro, V. Área de Protecção do Recurso Hidromineral das Termas de Entre-os-Rios. In Proceedings of the XI Congresso Brasileiro de Águas Subterrâneas, Fortaleza, Brazil, 15 September 2000; Available online: <https://aguassubterraneas.abas.org/asubterraneas/article/view/24343> (accessed on 25 January 2022). (In Portuguese).
65. Portaria n.º 203/2003 de 7 de Março. Establishes the Perimeter of Protection of Natural Mineral Water Corresponding to the Registration Number HM-23 and the Denomination of Entre-os-Rios (Quinta da Torre). Diário da República n.º 56, Série I-B 2003, Lisboa, Portugal. Available online: <https://data.dre.pt/eli/port/203/2003/03/07/p/dre/pt/html> (accessed on 5 February 2022).
66. Dias, G.; Noronha, F.; Ferreira, N. Introduction. In *Variscan Plutonism in the Central Iberian Zone, Northern Portugal, Eurogranites, Field Meeting*; Dias, G., Noronha, E., Ferreira, N., Eds.; Universidade do Minho, Escola de Ciências, Faculdade de Ciências da Universidade do Porto, Instituto Geológico e Mineiro: Porto, Portugal, 2000; pp. 7–26.
67. Pereira, E.; Ribeiro, A.; Carvalho, G.; Noronha, F.; Ferreira, N.; Monteiro, J. *Portugal's Geological Map, Scale 1/200000*; Paper 1; Serviços Geológicos de Portugal: Lisboa, Portugal, 1989. (In Portuguese)
68. Teixeira, J. Hidrogeomorfologia e Sustentabilidade de Recursos Hídricos Subterrâneos. Ph.D. Thesis, University of Aveiro, Aveiro, Portugal, 2011. Available online: <http://hdl.handle.net/10773/8308> (accessed on 5 February 2022). (In Portuguese).
69. Medeiros, A.; Pereira, E.; Moreira, A. *Portugal's Geological Map, scale 1/50.000*; Paper 9-D (Penafiel); Serviços Geológicos de Portugal: Lisboa, Portugal, 1981. (In Portuguese)
70. LAIST. *Relatório de Análise Físico-Química Completa—Fundação Inatel, Furo dos Barbeitos, Situado em Quinta da Torre, Entre-os-Rios*; Laboratório de Análises, Instituto Superior Técnico de Lisboa: Lisboa, Portugal, 2018. (In Portuguese)
71. LNEC. *Análise e Parecer Sobre a Situação Originada Pelo Derrame de Hidrocarbonetos em Entre-os-Rios*; Technical Report; Laboratório Nacional de Engenharia Civil: Lisboa, Portugal, 2008. (In Portuguese)
72. Bonham-Carter, G.F. *Geographic Information Systems for Geoscientists: Modelling with GIS*; Pergamon: Oxford, UK, 1994.
73. Sinan, M.; Razack, M. An Extension to the DRASTIC Model for Assessing Groundwater Vulnerability to Pollution: Application to the Haouz Aquifer of Marrakech (Morocco). *Environ. Geol.* **2008**, *57*, 349–363. [CrossRef]
74. DGT. Carta de Uso e Ocupação do Solo Para 2018. 2019. Available online: <http://mapas.dgterritorio.pt/wms-inspire/cos2018v1?service=WMS&REQUEST=GetCapabilities&VERSION=1.3.0> (accessed on 8 February 2022). (In Portuguese).
75. Singhal, B.; Gupta, R. *Applied Hydrogeology of Fractured Rocks*, 3rd ed.; Springer: Dordrecht, The Netherlands, 2010. [CrossRef]
76. LNEG. *Portugal's Geological Map, Scale 1:50 000*. 1981. Available online: [https://geoportal.lneg.pt/pt/dados\\_abertos/cartografia\\_geologica/cgp50k/](https://geoportal.lneg.pt/pt/dados_abertos/cartografia_geologica/cgp50k/) (accessed on 8 February 2022). (In Portuguese).
77. LNEC. *Cartografia da Vulnerabilidade à Poluição das Águas Subterrâneas do Concelho de Montemor-o-Novo Utilizando o Método DRASTIC. Proc. In 607/1/14252*; LNEC—Laboratório Nacional de Engenharia Civil, Departamento de Hidráulica, Grupo de Investigação de Águas Subterrâneas: Lisboa, Portugal, 2002; 53p. (In Portuguese)